NASA Technical Paper 1923

An Algorithm for Minimum-Cost Set-Point Ordering in a Cryogenic Wind Tunnel

John S. Tripp

NOVEMBER 1981

NASA

NASA Technical Paper 1923

An Algorithm for Minimum-Cost Set-Point Ordering in a Cryogenic Wind Tunnel

John S. Tripp
Langley Research Center
Hampton, Virginia

INTRODUCTION

Cryogenic wind tunnels, which use liquid nitrogen (LN_2) as a coolant, can be expensive to operate if controlled inefficiently because of the high cost of LN_2. In order to minimize operating expense, it is important that a cryogenic tunnel be equipped with a control system which accomplishes the following:

1. Establishes steady-flow conditions rapidly

2. Follows the most efficient transition path from one steady-flow setting to the next

3. Maintains steady flow at the most efficient setting during dwell at steady-state conditions for data acquisition

Of great importance is the need to sequence the test conditions (steady-flow settings, or set points) in time so that the total energy consumed during state transitions is minimized for all such sequences possible. This paper develops a simple, idealized model of the cryogenic-wind-tunnel process for evaluation of state-transition costs and an operational technique for determining the least expensive ordering of set points of all possible orderings. Some minimum-cost state-transition control strategies are identified and used where applicable for cost evaluation. Also, some numerical results using National Transonic Facility (NTF) test parameters to determine various set-point orderings are presented.

BACKGROUND

Minimum-energy, test-direction strategies for cryogenic wind tunnels have been studied by Balakrishna (ref. 1). A technique is developed in this reference for sequencing cryogenic-wind-tunnel set points which establishes tunnel operating parameters necessary for minimum coolant consumption at steady flow. A test-direction parameter is defined which enables minimum-cost ordering of a sequence of test points based on minimizing steady-flow coolant consumption. This paper develops an ordering technique based on transition dynamics rather than the static approach of Balakrishna. George Gumas of Pennsylvania State University, Middletown, Pennsylvania, (private communication) has investigated optimum dynamic-transition paths in cryogenic wind tunnels which minimize consumed energy and transition times. Gumas computes optimum coolant- and venting-flow rates for various linear transition-path directions based on a single-volume dynamic model of the cryogenic thermodynamics. The preliminary work of Gumas is extended in this paper.

APPROACH TO SET-POINT ORDERING

In this paper a set point s for a cryogenic wind tunnel (to be defined formally later) is a set of any three functionally independent steady-flow values of the process fluid-dynamic properties which uniquely define a steady-flow operating state. (A list of symbol definitions follows the references.) As an example, let

$$s = (T, p, M) \tag{1}$$

where T is static temperature, p is static pressure, and M is Mach number. A collection of n set points to be ordered is an indexed set S so that

$$S = \left\{ s_1, s_2, \ldots, s_n \right\} \tag{2}$$

For notational convenience the index set I_S of S (the set of indices in S) is defined as

$$I_S = \left\{ 1, 2, \ldots, n \right\} \tag{3}$$

A transition from set point s_i to set point s_j is the time history of the process as it is driven under external control from steady-flow state s_i to steady-flow state s_j. The transition from s_i to s_j will be represented notationally by the ordered pair (i,j). The transition set Ω of S is defined as the set of all $n(n-1)$ ordered pairs of elements of I_S so that

$$\Omega = \left\{ (i,j) : i,j \in I_S \text{ and } i \neq j \right\} \tag{4}$$

A closed tour Θ of S is an ordered subset of Ω containing n ordered pairs (transitions) so that

$$\Theta = \left\{ (i_1, i_2), (i_2, i_3), \ldots, (i_{n-1}, i_n), (i_n, i_1) \right\} \tag{5}$$

such that each element of I_S appears once and only once, both as a first element and as a second element of a pair in Θ. For each pair in Θ, the first element equals the second element of the preceding pair. Thus, a closed tour represents a set of transitions between the elements of S such that each element contained in S is visited once and only once, and the final transition returns to the initial element. An open tour Θ_o, a subset of Ω containing $n-1$ pairs, visits each state once and only once remaining in the final state without returning to the initial state, as indicated in the following:

$$\Theta_o = \left\{ (i_1, i_2), (i_2, i_3), \ldots, (i_{n-1}, i_n) \right\} \tag{6}$$

For each element (i,j) of the transition set Ω we compute the transition cost between states s_i and s_j (denoted by c_{ij}) by solving the differential equations of flow developed subsequently. A transition path giving the minimum transition cost is used when known. The resulting set of c_{ij} is ordered into a transition-cost matrix C, for which i denotes row and j denotes column. Note that diagonal elements of C will be null since transitions from state i to itself are not of interest.

The cost J_Θ of tour Θ is given by the following:

$$J_\Theta = \Sigma \, c_{ij} \qquad\qquad (i,j \in \Theta) \qquad\qquad (7)$$

The optimum set-point ordering of S then corresponds to the tour Θ^* for which the cost J_Θ^* is minimum over all possible tours.

DYNAMIC MODEL OF FLOW PROCESS

Model Requirements

Accurate mathematical representation of unsteady fluid flow in a tube of varying cross-sectional area requires computer solution of the Navier-Stokes partial differential equations. A one-dimensional model of the National Transonic Facility (NTF) wind tunnel based on the Navier-Stokes equations has been developed by the author for an ultra-high-speed vector-processing digital computer. It requires an execution duration approximately 11 times the real-time interval being simulated. Consider an example having 10 set points to be ordered for which the average transition time is 100 sec. The vector-processing time necessary to evaluate the 90-element transition-cost matrix using the previously described model would be 27.5 hr. Gumas (ref. 2) has developed an eight-volume lumped model of the NTF wind tunnel which, with simplification, could execute at a real-time rate on a high-speed serial digital computer. The 10-set-point example would then require 2.5 hr of machine time for evaluation of 90 transition costs. Clearly neither of these models could be employed in a practical set-point ordering algorithm because of slow execution rates. Drastic simplifications are required in modeling of flow for transition-cost evaluation. Simulation studies with both the Navier-Stokes and the Gumas models with feedback controls included show that Mach number transition settling times are always less than 15 sec, whereas temperature- and pressure-transition times are roughly proportional to the magnitude of the parameter change and in most cases exceed 15 sec. Therefore, an ordering algorithm which assigns priority to Mach number transitions at fixed pressure and temperature over pressure and temperature transitions at fixed Mach number would rarely incur serious inefficiencies. Furthermore, since such an algorithm would not require cost evaluation of Mach number transitions, Mach number dynamics could be neglected in the process model. As a result, temperature and pressure dynamics, which depend primarily on global values of mass and energy, could be described by a single-volume lumped model. This would permit the desired model simplification. Another advantage of neglecting Mach number dynamics is the consequent reduction in the number of set-point transition costs through which the operational ordering algorithm must search. As will be shown, search time increases rapidly with the number of set points. Although the single-volume lumped model and analytic transition paths are idealizations of the real world, they are adequate for purposes of set-point ordering.

Equations of State

The equations of state for a single-volume lumped model of a cryogenic wind tunnel are now developed. The two state variables are total mass m and total internal energy e. A state is defined as the pair (m,e). There are three control variables:

w_N LN_2 flow rate

w_G gas-vent flow rate

P   fan power

The differential equations of state are thus given by

$$\dot{m} = w_N - w_G \tag{8}$$

and

$$\dot{e} = h_N w_N - h_G w_G + P \tag{9}$$

where h_N and h_G are the enthalpies of LN_2 and the vented gas. These equations account for the accumulated mass and energy in the closed system. Total internal energy e, including gas internal energy and heat energy stored in the metal tunnel liner, is given by the following:

$$e = c_v m T + c_s m_s T \tag{10}$$

where

T   absolute static temperature of gas and liner

c_v specific heat of gas at constant volume

m_s mass of tunnel liner

c_s specific heat of tunnel liner

Equation (10) is based on the assumption that tunnel-liner and gas temperatures are equal, which is actually true only for steady flow. Equation (9) assumes that the tunnel is insulated so that external heat transfer is negligible. Furthermore, the dynamic component of total energy is neglected. For convenience, we can define the variable a_s as the following:

$$a_s = \frac{c_s}{c_v} m_s \tag{11}$$

Then, from equations (10) and (11), temperature may be expressed by the following as a property dependent on state variables m and e:

$$T = \frac{e}{c_v (m + a_s)} \tag{12}$$

From the ideal-gas law and the definition of enthalpy, static pressure p and gas enthalpy h_G are expressed as functions of m and e by

$$p = K_a \frac{\gamma - 1}{V} \frac{me}{m + a_s} \tag{13}$$

and

$$h_G = \frac{\gamma e}{m + a_s} \tag{14}$$

where V is the tunnel volume, γ is the ratio of specific heats, and K_a is a constant.

Gumas (private communication), through experimentation, determined that Mach number M could be approximated by the following empirical relation:

$$M^2 = \frac{P}{K_m p_t \sqrt{T_t}} \tag{15}$$

where K_m is a constant and the subscript t indicates the total values of p and T. Mach number determined by this relation will be in error by less than 10 percent for a fan speed of 360 rpm and a temperature range of 111 K to 278 K. With little change in results, p_t and T_t may be replaced by static values, giving

$$M^2 = \frac{P}{K_m p \sqrt{T}} \tag{16}$$

which gives Mach number as a function of the state variables and input variable P.

Equations (12) and (13) may be solved simultaneously for m and e in terms of p and T, thus giving the following:

$$m = \frac{Vp}{K_a RT} \tag{17}$$

and

$$e = \frac{Vp}{K_a(\gamma - 1)} + a_s c_v T \tag{18}$$

where R is the gas constant. A set point defined in terms of state variables m and e is the following:

$$s = (m, e, M) \tag{19}$$

where m and e are steady-flow values. Accordingly,

$$\dot{m} = 0 \tag{20}$$

and

$$\dot{e} = 0 \tag{21}$$

With equations (12), (13), and (16), the set point determines the value of P for steady flow. Likewise, with equations (8), (9), (20), and (21), it determines the required values of w_G and w_N for steady flow. A set point may be expressed in terms of any three functionally independent properties such as static pressure p, static temperature T, dynamic pressure q, Reynolds number N_{Re}, or density ρ. The following relations along with equations (12) and (13) may be used for determining the values of these properties:

$$\rho = \frac{p}{K_a RT} \tag{22}$$

$$q = \frac{1}{2}\gamma p M^2 \tag{23}$$

and

$$N_{Re} = \frac{\rho \bar{c}}{\mu} M \sqrt{\gamma RT} \tag{24}$$

where $\bar{c}$ is reference length and μ is viscosity. In the examples given later, set points are given in (T, p, M) form.

A state transition from set point (m_1, e_1, M_1) to set point (m_2, e_2, M_2) is produced by a transition control law L as follows:

$$L = \left(w_N(t), w_G(t), P(t) \right) \tag{25}$$

a triple of time functions defined over some time interval (t_1, t_2) such that

$$m_2 = \int_{t_1}^{t_2} \left[w_N(t) - w_G(t) \right] dt + m_1 \tag{26}$$

$$e_2 = \int_{t_1}^{t_2} \left[h_N w_N(t) - h_G(t) w_G(t) + P(t) \right] dt + e_1 \tag{27}$$

and

$$M_2 = \sqrt{\frac{P(t_2)}{K_m p_2 \sqrt{T_2}}} \tag{28}$$

The transition cost J_L of control law L is defined by

$$J_L = \int_{t_1}^{t_2} \left[P(t) + r w_N(t) \right] dt \tag{29}$$

6

where r is the cost of LN_2 relative to fan-energy cost. Note that L may be difficult to determine and may not be unique. The values of w_N, w_G, and P are subject to the following bounds:

$$0 \leq w_N \leq w_{N,max} \tag{30}$$

$$0 \leq w_G \leq w_{G,max} \tag{31}$$

and

$$P_{min} \leq P \leq P_{max} \tag{32}$$

(Upper limits on $|\dot{w}_N|$, $|\dot{w}_G|$, and $|\dot{P}|$, which are imposed in the NTF, are neglected here.) An optimum control law L^* is defined to be a control (among all controls which drive the process from set point s_1 to s_2 and satisfy inequalities (30) to (32)) which satisfies the following:

$$J_{L^*} \leq J_L \tag{33}$$

for all L.

A state-transition path under control law L for the time interval (t_1, t_2) from state (m_1, e_1) to state (m_2, e_2) is the locus of points described in the two-dimensional state space by the state variables $m(t)$ and $e(t)$, where

$$m(t) = \int_{t_1}^{t} \left[w_N(t) - w_G(t) \right] dt + m_1 \tag{34}$$

and

$$e(t) = \int_{t_1}^{t} \left[h_N w_N(t) - h_G(t) w_G(t) + P(t) \right] dt + e_1 \tag{35}$$

A state-transition path produced by an optimum control law is said to be an optimum path. For the remainder of the paper, the transition from state (m_1, e_1) to state (m_2, e_2) will for convenience be denoted by the ordered pair $(\Delta m, \Delta e)$, where

$$\Delta m = m_2 - m_1 \tag{36}$$

and

$$\Delta e = e_2 - e_1 \tag{37}$$

For some control law L, which produces a state transition from (m_1, e_1) to (m_2, e_2), equation (29) may be rewritten as follows by using equations (8) and (9) to eliminate w_N:

$$J_L = \int_{t_1}^{t_2} \left[\dot{e} + (r - h_N)\dot{m} + (h_G - h_N + r)w_G \right] dt$$

$$= \Delta e + (r - h_N)\,\Delta m + \int_{t_1}^{t_2} (h_G - h_N + r)w_G\, dt \qquad (38)$$

Equation (38) shows that J_L is determined by state increments (Δm, Δe) and by $w_G(t)$. It follows that any control L for which $w_G \equiv 0$ is optimum since Δe and Δm are fixed.

It is of interest to determine the region in state space about state (m_2, e_2) to which transitions can be made with $w_G \equiv 0$. Let $w_G \equiv 0$. From inequality (30) and equation (34),

$$\Delta m = \int_{t_1}^{t_2} w_N(t)\, dt \geq 0 \qquad (39)$$

From inequality (32) and equation (35),

$$\Delta e = h_N\,\Delta m + \int_{t_1}^{t_2} P(t)\, dt \geq h_N\,\Delta m + P_{min}\,\Delta t \qquad (40)$$

From inequalities (30) and (39),

$$0 \leq \Delta m = \int_{t_1}^{t_2} w_N(t)\, dt \leq w_{N,max}\,\Delta t \qquad (41)$$

so that

$$\Delta t \geq \frac{\Delta m}{w_{N,max}} \geq 0 \qquad (42)$$

Substituting inequality (42) into inequality (40) gives

$$\Delta e \geq \left(h_N + \frac{P_{min}}{w_{N,max}} \right) \Delta m \qquad (43)$$

8

Thus, necessary conditions for state transition $(\Delta m, \Delta e)$ to be realized with $w_G \equiv 0$ are inequalities (39) and (43).

Conversely, let conditions defined by inequalities (39) and (43) be satisfied, that is,

$$\Delta m' \geq 0 \tag{44}$$

and

$$\Delta e' \geq \left(h_N + \frac{P_{min}}{w_{N,max}} \right) \Delta m' \tag{45}$$

where the prime indicates particular values of Δm and Δe. Choose $w_G \equiv 0$ and $w_N = w_{N,max}$. From inequality (39) it follows that

$$\Delta t = \frac{\Delta m'}{w_{N,max}} \tag{46}$$

Also choose the following:

$$P = \left(\frac{\Delta e'}{\Delta m'} - h_{N,max} \right) w_{N,max} \geq P_{min} \tag{47}$$

From the equation part of inequality (40) it follows that

$$\Delta e = h_N \, \Delta m' + \left(\frac{\Delta e'}{\Delta m'} - h_N \right) w_{N,max} \, \Delta t = \Delta e' \tag{48}$$

Thus, inequalities (39) and (43) are also sufficient conditions for state transition $(\Delta m', \Delta e')$ to be realized with $w_G \equiv 0$.

To summarize, necessary and sufficient conditions for state transition $(\Delta m, \Delta e)$ to be realized with $w_G \equiv 0$ and satisfying conditions (30) and (32) are

$$\Delta m \geq 0 \tag{39}$$

and

$$\Delta e \geq \left(h_N + \frac{P_{min}}{w_{N,max}} \right) \Delta m \tag{43}$$

It is shown in the appendix that a transition control L in which $w_N \equiv 0$ is locally optimum in the sense that along a fixed transition path between (m_1, e_1) and (m_2, e_2) any positive variation $\delta w_N(t)$ about $w_N \equiv 0$ causes a positive increase in

transition cost J over its value for $w_N \equiv 0$. The region in state space from which transitions can be made to state (m,e) with $w_N \equiv 0$ is now determined. Let $w_N \equiv 0$. From inequality (31) and equation (34),

$$\Delta m = -\int_{t_1}^{t_2} w_G(t) \; dt \leq 0 \tag{49}$$

and from equation (35),

$$\Delta e = \int_{t_1}^{t_2} \left[-h_G(t) w_G(t) + P(t) \right] dt \tag{50}$$

The enthalpy h_G is bounded as follows:

$$c_p T_{min} \leq h_G(t) \leq c_p T_{max} \tag{51}$$

From inequalities (49) and (31),

$$\Delta t \geq -\frac{\Delta m}{w_{G,max}} \geq 0 \tag{52}$$

From equation (50) and inequalities (31), (51), and (52),

$$\Delta e \geq \left(-c_p T_{max} w_{G,max} + P_{min} \right) \Delta t \geq \left(c_p T_{max} - \frac{P_{min}}{w_{G,max}} \right) \Delta m \tag{53}$$

Thus, necessary conditions for state transition $(\Delta m, \Delta e)$ to be realized with $w_N \equiv 0$ are inequalities (49) and (53).

Next, let the conditions defined by inequalities (49) and (55) be satisfied, that is,

$$\Delta m' \leq 0 \tag{54}$$

and

$$\Delta e' \geq \left(c_p T_{min} - \frac{P_{min}}{w_{G,max}} \right) \Delta m' \tag{55}$$

Set $w_N \equiv 0$, $w_G = w_{G,max}$, and

$$P = \left(c_p T - \frac{\Delta e}{\Delta m'} \right) w_{G,max} \geq P_{min} + (T - T_{min}) w_{G,max} > P_{min} \tag{56}$$

10

From inequality (54),

$$\Delta t = - \frac{\Delta m'}{w_{G,max}} \tag{57}$$

and from equation (35),

$$\Delta e = \int_{t_1}^{t_2} \left[-c_p T w_{G,max} + \left(c_p T - \frac{\Delta e'}{\Delta m'} \right) w_{G,max} \right] dt = \Delta e' \tag{58}$$

Thus, inequalities (49) and (55) are sufficient conditions for state transition $(\Delta m', \Delta e')$ to be realized with $w_N \equiv 0$.

Summarizing, conditions for state transition $(\Delta m, \Delta e)$ to be realized with $w_N \equiv 0$ and satisfying conditions (31) and (32) are as follows:

$$\Delta m \leq 0 \tag{49}$$

and

$$\Delta e \geq \left(c_p T_{max} - \frac{P_{min}}{w_{G,max}} \right) \Delta m \tag{53}$$

or

$$\Delta e \geq \left(c_p T_{min} - \frac{P_{min}}{w_{G,max}} \right) \Delta m \tag{55}$$

Inequalities (49) and (53) taken together constitute necessary conditions, whereas inequalities (49) and (55) taken together constitute sufficient conditions.

It has not been proven that controls with $w_N \equiv 0$ are globally optimum over their regions of admissibility. However, computational experience did not reveal any controls less expensive than those with $w_N \equiv 0$ for a given transition. In order to develop the curves in figure 1, inequalities (39), (43), (49), and (55) are rewritten in terms of m_1, e_1, m_2, and e_2. For $w_G \equiv 0$,

$$m_1 \leq m_2 \tag{59}$$

and

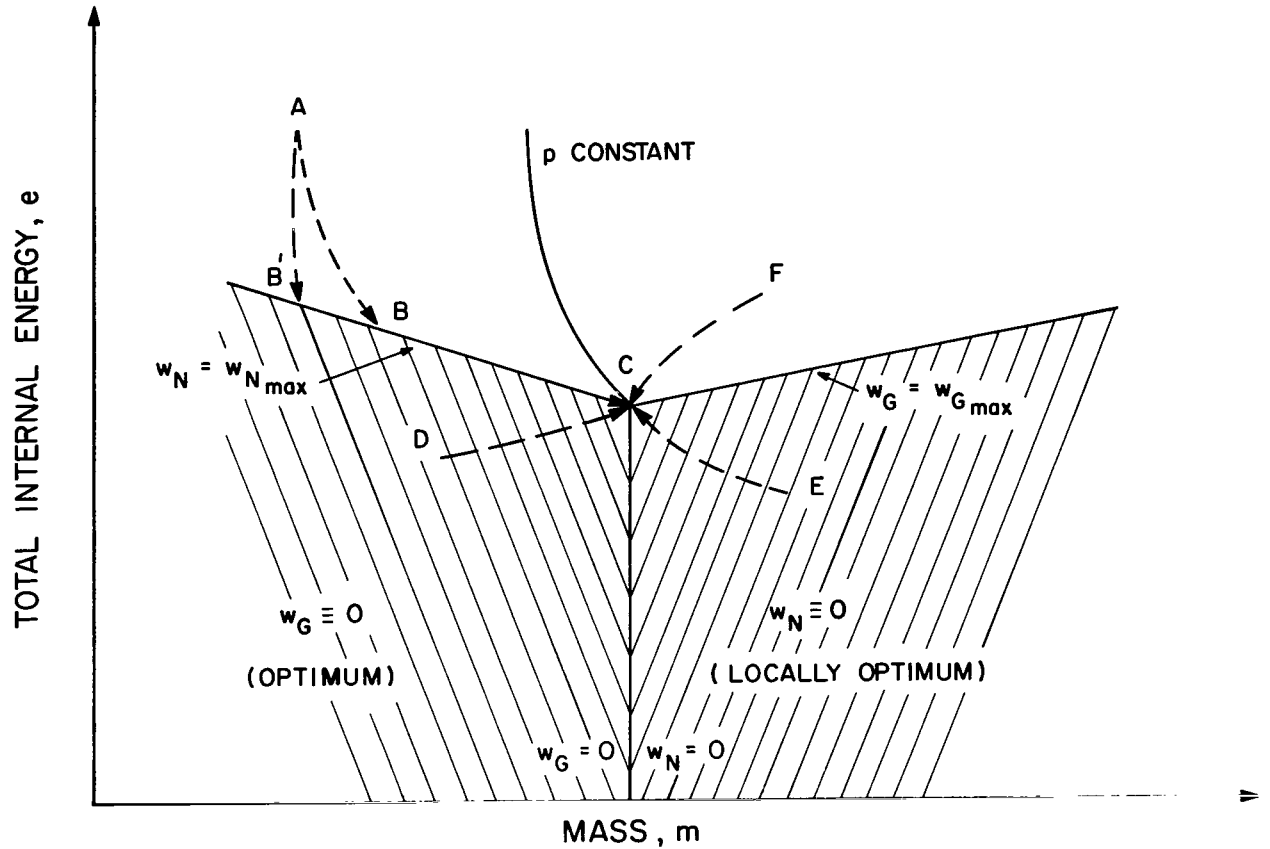$$e_1 \leq e_2 + \left(h_N + \frac{P_{min}}{w_{N,max}} \right) (m_1 - m_2) \tag{60}$$

Figure 1.- Transition-path regions in mass-energy plane.

For $w_N \equiv 0$,

$$m_1 \overset{\geq}{} m_2 \tag{61}$$

and

$$e_1 \leq e_2 + \left(c_p T_{min} - \frac{P_{min}}{w_{G,max}} \right) (m_1 - m_2) \tag{62}$$

The regions defined by inequalities (59) to (62) appear in figure 1, in which point C represents terminal state (m_2, e_2) in the mass-energy plane. The shaded area labeled $w_G \equiv 0$ represents the set of initial states (m_1, e_1) from which state (m_2, e_2) can be reached with controls having $w_G \equiv 0$ (defined by inequalities (59) and (60)). Similarly, the area labeled $w_N \equiv 0$ represents the set of initial states from which (m_2, e_2) can be reached with $w_N \equiv 0$ (defined by inequalities (61) and (62)). Figure 2 shows the regions of figure 1 mapped into the temperature-pressure plane.

Figure 2.- Transition-path regions in temperature-pressure plane.

Outside the optimum and locally optimum regions of figures 1 and 2, precise determination of optimum controls would require the use of techniques such as the minimum principle or dynamic programming (ref. 3), involving extensive computational requirements. After preliminary investigation of the minimum principle did not disclose any simple optimum control strategies for the cases which require its application, numerical parametric studies were performed to experimentally discover the best transition paths, which led to the following strategies:

Case I - decreasing temperature and increasing pressure. As shown in path ABC of figure 2, cool the tunnel at constant pressure to the boundary of the $w_G \equiv 0$ region, then cool and pressurize with $w_G \equiv 0$ to the terminal set point C. Additional reduction in transition cost is obtained along path AB'C. However, the pressure decrease along segment AB' followed by a pressure increase along segment B'C would be undesirable in actual wind-tunnel operations. Therefore, path ABC is preferred to AB'C.

Case II - decreasing temperature and decreasing pressure. Since experimental numerical studies did not reveal any preferred paths in this region, arbitrary straight lines are followed in the temperature-pressure plane for convenience, as illustrated by path FC in figure 2.

For computational convenience linear paths are also followed in the $w_G \equiv 0$ and $w_N \equiv 0$ regions, as shown by paths DC and EC in figure 2. Paths ABC, FC, DC, and EC mapped into the mass-energy plane are shown in figure 1. Controls actually used in an automated cryogenic wind tunnel may be substituted for those developed herein.

The control logic required to follow a direct path in the temperature-pressure plane between initial state (T_1, p_1) and final state (T_2, p_2) is now presented. The equation of a linear path is

$$p = p_1 - \frac{\Delta p}{\Delta T} T_1 + \frac{\Delta p}{\Delta T} T = a + \lambda T \tag{63}$$

where

$$a = p_1 - \frac{\Delta p}{\Delta T} T_1 \tag{64}$$

and

$$\lambda = \frac{\Delta p}{\Delta T} \tag{65}$$

Substituting equation (63) into equations (17) and (18) gives the following expressions for m and e as functions of T:

$$m = \frac{V}{K_a R T}(a + \lambda T) \tag{66}$$

and

$$e = \frac{Va}{K_a(\gamma - 1)} + \left[\frac{V\lambda}{K_a(\gamma - 1)} + a_s c_v \right] T \tag{67}$$

Differentiating equations (66) and (67) gives

$$\dot{m} = \frac{Va}{K_a R T^2} \dot{T} \tag{68}$$

and

$$\dot{e} = \left[\frac{V\lambda}{K_a(\gamma - 1)} + a_s c_v \right] \dot{T} \tag{69}$$

Equations (8), (9), (68), and (69) are solved simultaneously to eliminate $\dot{m}$, $\dot{e}$, and $\dot{T}$, giving w_G as a function of w_N, P, and T as follows:

$$w_G = w_N + \left[\frac{(h_N - c_p T) w_N + P}{GT^2 + c_p T} \right] \tag{70}$$

14

where

$$G = \frac{RK_a}{Va}\left(\frac{v\lambda}{\gamma - 1} + a_s c_v\right) \tag{71}$$

Alternatively, w_N may be obtained as a function of w_G, P, and T to give

$$w_N = w_G - \left[\frac{(h_N - c_pT)w_G + P}{GT^2 + h_N}\right] \tag{72}$$

Equations (70) and (72) are in a form suitable for implementing a state-variable feedback control law. For example, if w_N is to be the independent control variable, it is chosen arbitrarily within the bounds of inequality (30). Mach number M, also chosen arbitrarily, must be such that P remains within the bounds of inequality (32). Since state variables m and e are known for all times during a controlled state transition, T is obtained from equation (12). At each stage of the controlled transition the required value of control variable P is obtained from equations (12), (13), and (16), and the required value of w_G is computed from equation (70). Similarly, if w_G is the independent control variable, it must satisfy inequality (31). The required values of w_N are then obtained from equation (72).

For transitions occurring within the shaded region of figure 2 labeled $w_G \boxminus 0$ (or $w_N \equiv 0$), w_G (or w_N) is selected as the independent control variable and set to zero. The required value of w_N (or w_G) is computed from equation (72) (or eq. (70)). Outside both shaded regions of figure 2, w_N is selected as the independent control variable and is made as large as possible to minimize transition time while maintaining itself and w_G within the bounds of inequalities (30) and (31). If inequality (31) is violated, w_G is selected as the independent control variable instead. Mach number is chosen large (0.8) for transition directions of increasing energy and small (0.3) for directions of decreasing energy, also to minimize transition time.

Equations (70) and (72) are invalid for constant-temperature transitions since the slope λ becomes infinite. For increasing pressure at constant temperature, w_G is set to zero and w_N is computed using the following:

$$w_N = \frac{P}{c_v T - h_N} \tag{73}$$

which is obtained by differentiating equations (17) and (18), setting $\dot{T}$ to zero, and eliminating $\dot{m}$ and $\dot{e}$ as was done for equations (70) and (72). For decreasing pressure at constant temperature, w_N is made independent (set to zero when possible) and w_G is computed from the following:

$$w_G = \frac{(h_N - c_vT)w_N + P}{RT} \tag{74}$$

OPTIMUM TOUR GENERATION

The Traveling Salesman Problem

Consider a set S of n set points. From this we can generate a transition-cost matrix C by using the dynamic-flow model and transition-control logic developed previously, with the diagonal elements set to infinity. The problem is to determine the optimum tour $\Theta*$ having the least cost $J_{\Theta}*$. This problem is identified in the mathematical programming literature as the "traveling salesman problem" (TSP), wherein a salesman is to visit each of n cities only once, beginning and ending at the same city. The problem involves the order in which he should tour the cities to minimize the total distance traveled. Since there are $(n - 1)!$ possible tours, enumeration is a feasible method of solution only for small n.

The TSP is termed symmetric or asymmetric depending on whether C is symmetric or asymmetric. Various techniques for exact solution of both symmetric and asymmetric TSP's appear in the literature, including dynamic programming, integer programming, and branch and bound methods. In addition, numerous approximate methods exist which are not considered here.

Dynamic-programming algorithms (described in ref. 4) perform well for small n (less than 13). However, computer storage requirements become excessive as n increases.

The TSP may be cast as a linear-programming problem having integer values 0 and 1 and $2^{n-1} - 1$ constraints. Various techniques based on this approach have been developed. According to Bellmore and Nemhauser (ref. 4) the performance of integer-programming algorithms varies widely from problem to problem. Execution time grows rapidly with increasing n.

The branch and bound methods appear to offer the best performance. Earlier versions of branch and bound developed by Little et al. (ref. 5) and Shapiro (cited in ref. 4) are reviewed favorably by Bellmore and Nemhauser (ref. 4). Little's method, which is simple to program, is used in the work reported herein. It offers adequate performance without excessive storage requirements for $n < 40$, although reference 5 cautions that solution time increases exponentially with n. Later extensions of branch and bound methods such as the restricted Lagrangian approach of Balas and Christofides (ref. 6) provide superior performance for large n. For example, this method solves a 375-node problem in less than 82 sec, whereas a 100-node problem executes in an average of 0.7 sec on a large serial digital computer. Such a high-performance algorithm might be employed in a production version of a set-point ordering package, but it was not required for the study reported herein.

Branch and Bound Algorithm

A brief description of Little's branch and bound method is now given. The procedure is to partition the set of all tours by constructing a binary tree structure, each node of which represents a set of tours either containing or excluding some particular transition. We then compute a lower bound on the costs of the tours contained in each node. At each stage of the decomposition, the node whose omission would be the most expensive is decomposed and new lower bounds are computed for the decomposition. It is shown in figure 3 that from the root of the tree, which represents the set of all tours, there are two branches: Node 1 (to the left) represents the set of
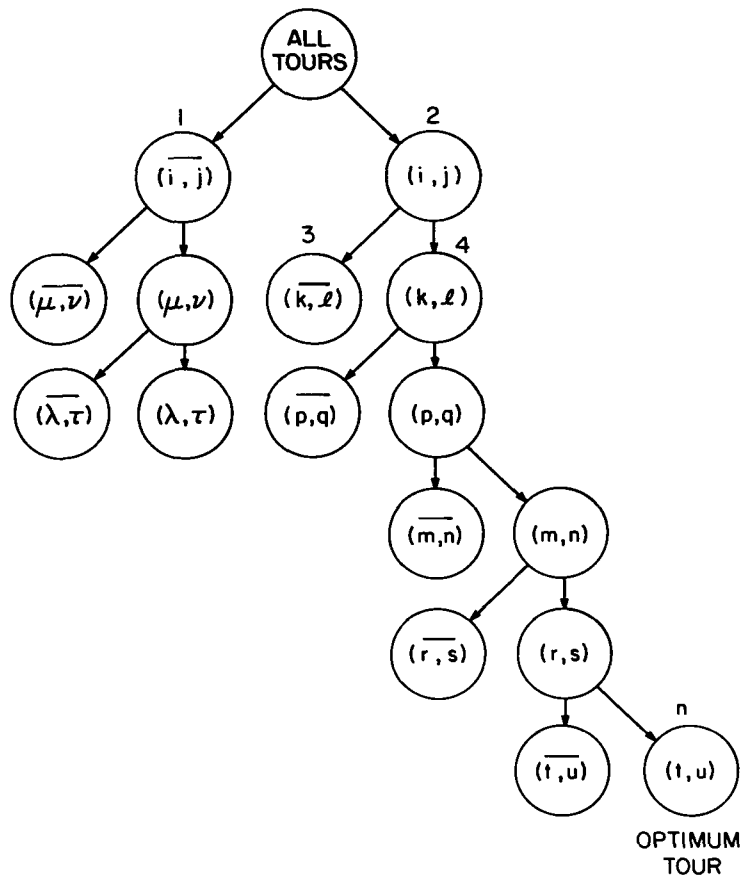
Figure 3.- Branch and bound decomposition. A bar over an ordered
pair indicates exclusion of that pair.

tours excluding transition (i,j), denoted by $\overline{(i,j)}$; node 2 (to the right) represents
the set of tours containing transition (i,j). (The letter symbols used in this
figure represent integers.) Node 3, the left subnode below node 2, represents the
set of tours containing transition (i,j) and excluding transition (k,ℓ). Node 4
represents the set of tours including transitions (i,j) and (k,ℓ). The decomposition
continues in a like manner as illustrated in the figure. A node is terminal if no
more transitions may be excluded; the set of transitions contained in a terminal node
represents a single tour. Terminal node n in figure 3, for example, contains
transitions (i,j), (k,ℓ), (p,q), (m,n), (r,s), and (t,u). A path is pursued only as
long as its current lower bound remains less than all other lower bounds in the tree.
Otherwise, the path is abandoned and the search resumes at the node having the least
lower bound. An optimal tour has been found when a terminal node is reached whose
true cost is less than or equal to every other lower bound computed in the tree.

A lower bound on the costs of the set of all tours is obtained by reduction of
the transition-cost matrix C. A row (or column) is reduced by subtracting its small-
est element from each element in the row (or column). A matrix is reduced if all
elements are nonnegative and if each row and each column contain at least one zero.
The sum of elements required to reduce every row and column in C is a lower bound

on the costs of the set of all tours. Suppose the search has reached node (i,j). Based on decision logic described later, a branch is constructed from node (i,j) to node (k,ℓ), and row k and column ℓ are deleted from C to form a new matrix C'. Matrix C' is then reduced, and the lower bound at node (k,ℓ) equals the lower bound at (i,j) plus the sum of the reducing elements of C'. The lower bound of node $\overline{(k,\ell)}$, equals the sum of the lower bound at (i,j) and $\theta(k,\ell)$, defined as the sum of the smallest cost in row k and the smallest cost in column ℓ. To determine (k,ℓ), $\theta(k,\ell)$ is computed for each position in C' and a branch is made to the node (k,ℓ) for which $\theta(k,\ell)$ is the largest. This strategy favors transitions whose exclusion would increase the cost of a tour most rapidly.

At each step of the branching process transitions must be excluded from a path which would produce subtours, that is, transitions to any state already included in the partially constructed tour. Such transitions are eliminated by setting their transition costs to infinity in the reduced cost matrix. Thus, many potential dead-end search paths are eliminated. A complete tour has been determined when C is reduced to a 2 by 2 matrix.

Little's algorithm is explained fully in reference 5. An example of a branch and bound solution to the TSP is given in Whitehouse and Wechsler (ref. 7). More formal expositions of branch and bound algorithms appear in Henley and Williams (ref. 8) and in Garfinkel and Nemhauser (ref. 9).

NUMERICAL PERFORMANCE OF SET-POINT-ORDERING ALGORITHM

Digital Computer Program

A digital computer program has been written which combines a single-volume fluid-flow model, transition-path control logic, and a branch and bound tour-generating algorithm, all as previously described, into a set-point ordering package. It was found that a variable-order, variable-step-size Adams method (ref. 10) for integrating the differential equations is ideal. After 6 to 10 starting steps during the first second of simulated time, the variable step size increases rapidly to as much as several hundred seconds. Most test cases involving simulated time durations up to 2000 sec execute in 25 steps or less. As a result, the total execution time required for transition-cost-matrix evaluation is a fraction of that required by the branch and bound algorithm.

The program accepts set points in the form of equation (1), that is,

$$s = (T,p,M)$$

For each combination of temperature T and pressure p, all associated values of Mach number M are ordered in ascending order. As discussed previously, transition costs are evaluated only for temperature-pressure transitions. Diagonal elements of matrix C are set to infinity.

Closed-Tour Performance

Several test examples based on NTF parameters are now discussed. Figure 4 shows six set points numbered in the temperature-pressure plane to indicate the ordering of an optimum closed tour (example 1). The arrows between the points, which in some

cases are schematic rather than actual transition-path loci, are labeled where applicable to indicate optimum transitions with $w_N \equiv 0$ or $w_G \equiv 0$. Note that the tour, a simple closed figure, contains four optimum transitions. The significantly lower cost of transitions with $w_N \equiv 0$ causes their high frequency of occurrence in all the cases studied.

A nine-set-point closed tour is shown in figure 5 in the same format (example 2). Note that the convoluted shape of the tour produces a preponderance of optimum transitions, six out of nine in this example. These set points were chosen to fill a rectangular region of the temperature-pressure plane rather than a realistic operating envelope.

A 12-set-point closed tour (example 3) is shown in figure 6. Nine of the 12 transitions are optimum, with $w_N \equiv 0$ in each of the 9 and w_G are zero in transition (8,9). Each of the three examples indicates that depressurization at constant temperature is highly favored by the algorithm because it is achieved with zero coolant consumption.
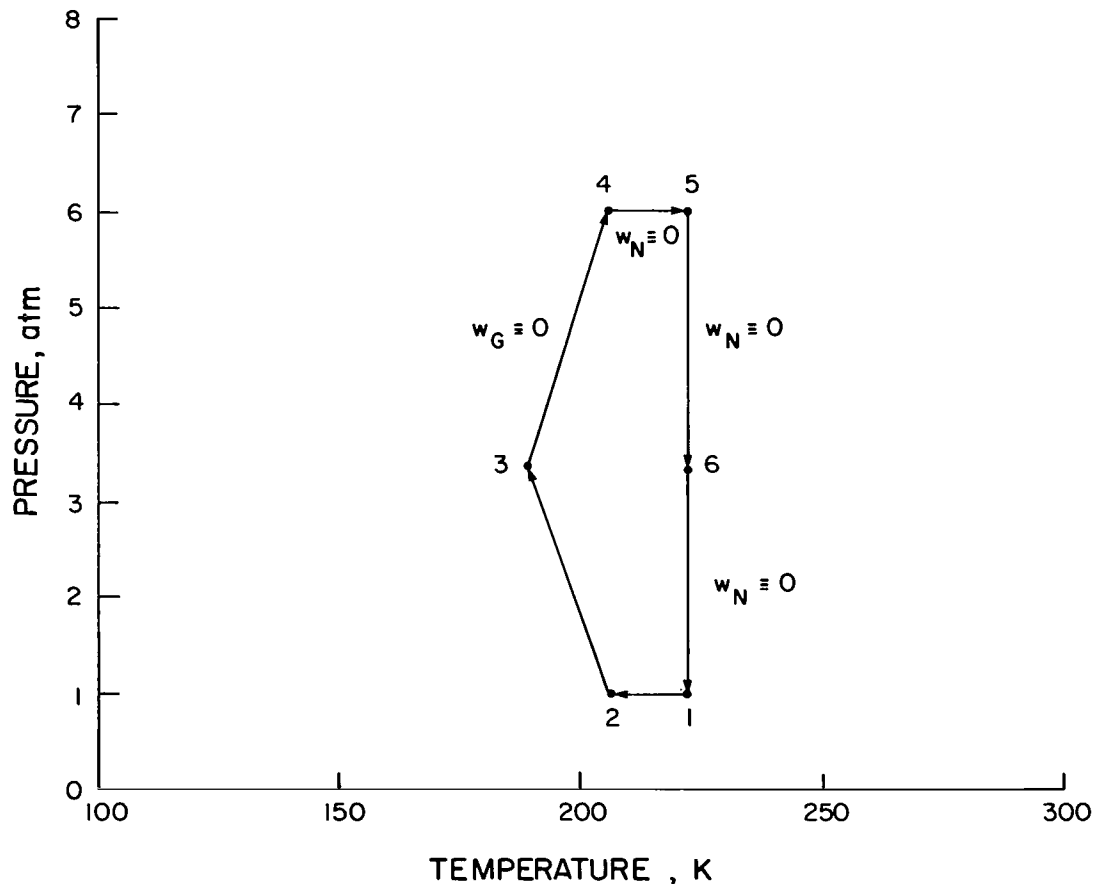

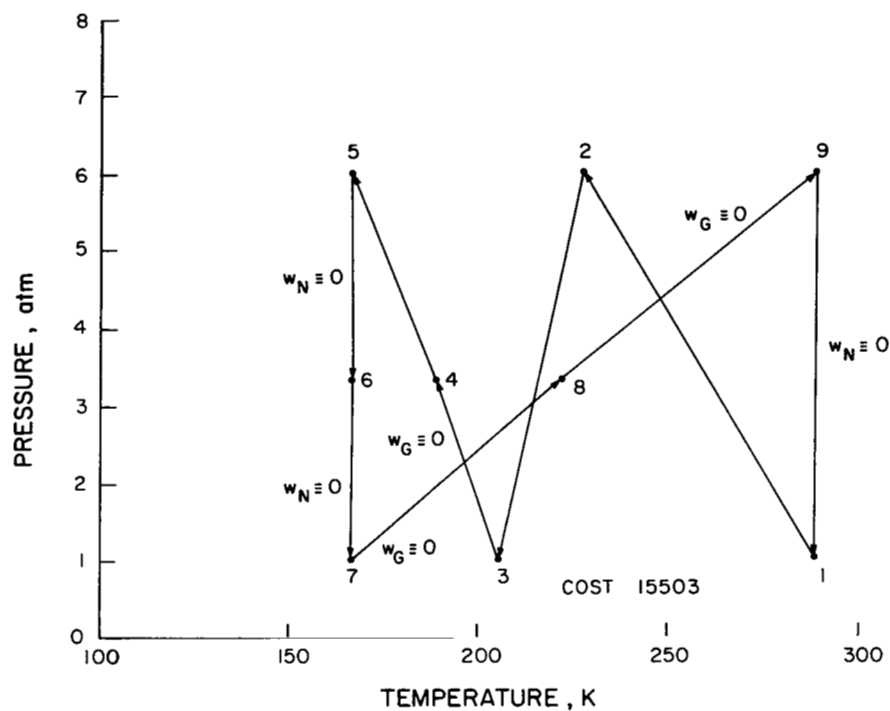Figure 4.- Six-set-point optimum closed tour.

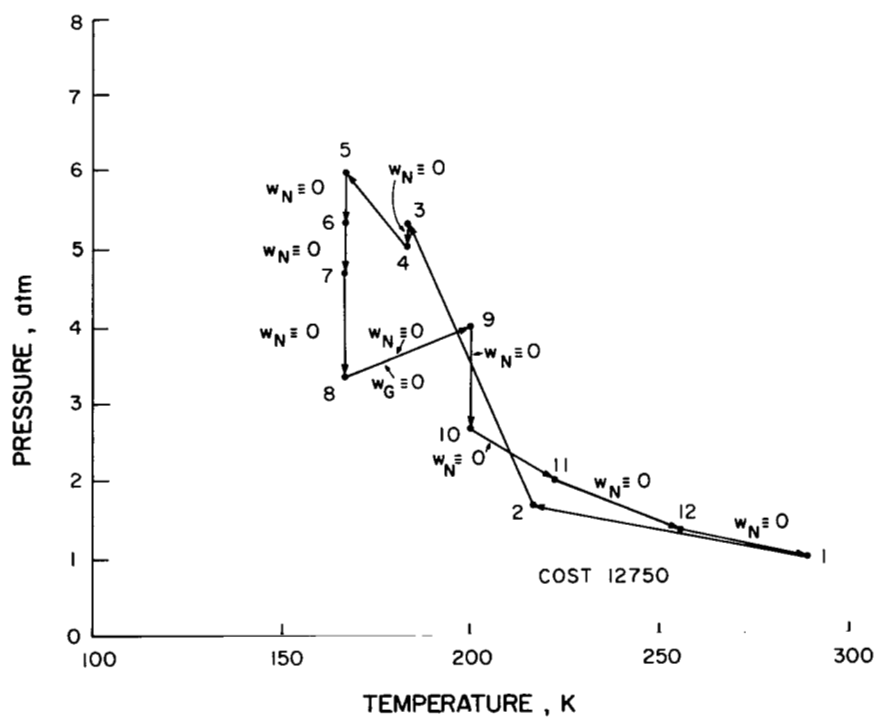Figure 5.- Nine-set-point optimum closed tour.

Figure 6.- Twelve-set-point optimum closed tour.

20

Open-Tour Performance

Two optional modes are provided in the program which generate optimum open tours as follows:

1. Determination of the best open tour with a free terminal set point

2. Determination of the best open tour with a fixed terminal set point

Mode 1 is implemented by setting the first column of matrix C to zero prior to execution of the branch and bound algorithm. This modification removes the cost of the final transition to set point 1 from the computation. The resulting closed tour is equivalent to the least expensive open tour.

To understand mode 2 operation, let set point k be the selected fixed terminal set point for an open tour. All of the elements of column 1 of C are set to infinity except element (k,ℓ) which is set to zero. This forces the final transition of an optimum closed tour to be from set point k to set point 1 at zero cost, which is equivalent to an optimum open tour terminating at set point k.

The nine-set-point optimum open tour with free terminal set point for example 2 data, shown in figure 7, has the same ordering as the optimum closed tour. Its cost is only slightly less than that of the closed tour. Figure 8 shows the optimum open tour for the same data ending at set point 2 (222 K, 6.0 atm), which forces a complete reordering of the set points at considerably greater cost.

Figures 9 to 11 illustrate open tours for the 12-set-point data of example 3. The 12-set-point optimum open tour with free terminal set point, shown in figure 9, is
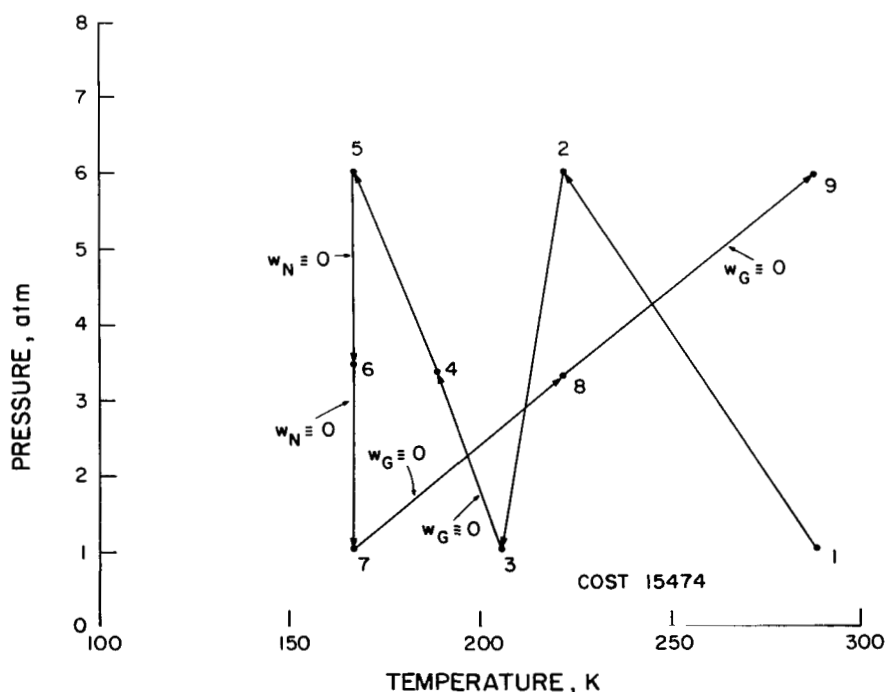

Figure 7.- Nine-set-point optimum open tour with
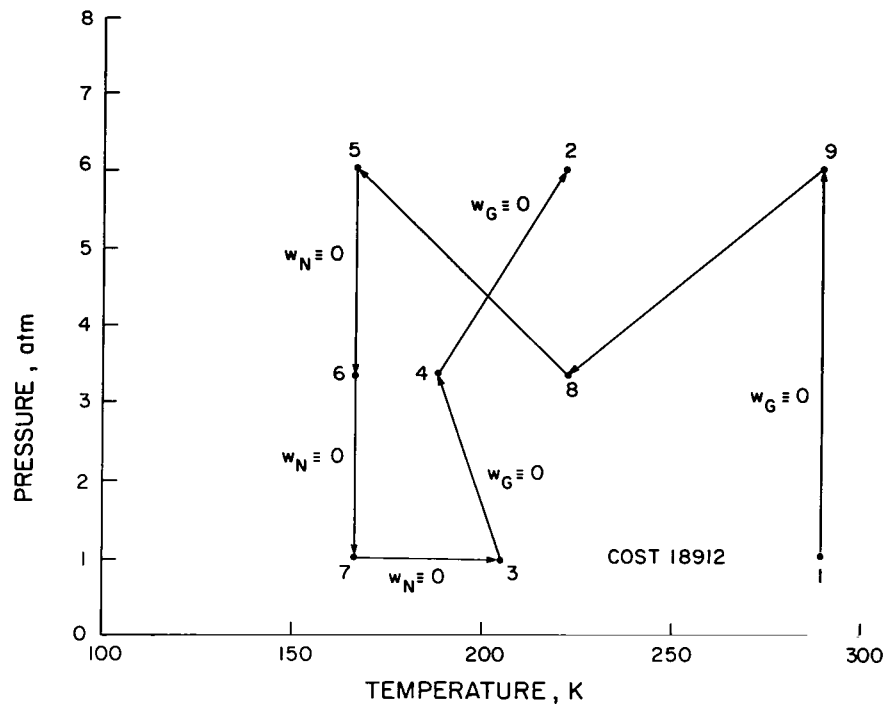free terminal set point (mode 1).

Figure 8.- Nine-set-point optimum open tour with
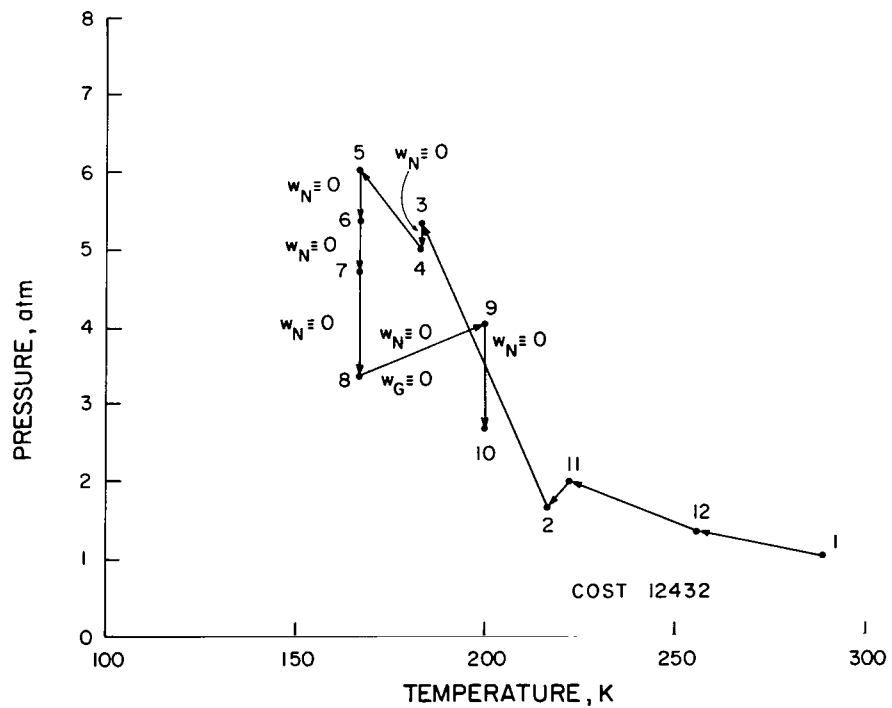fixed terminal set point (mode 2).

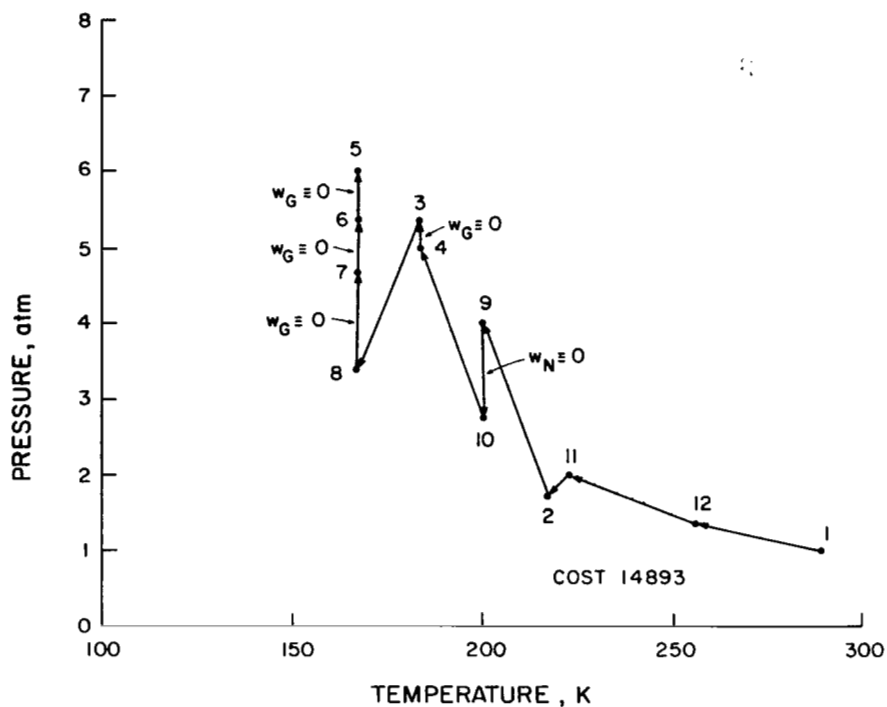Figure 9.- Twelve-set-point optimum open tour with
free terminal set point.

Figure 10.- Twelve-set-point optimum open tour with
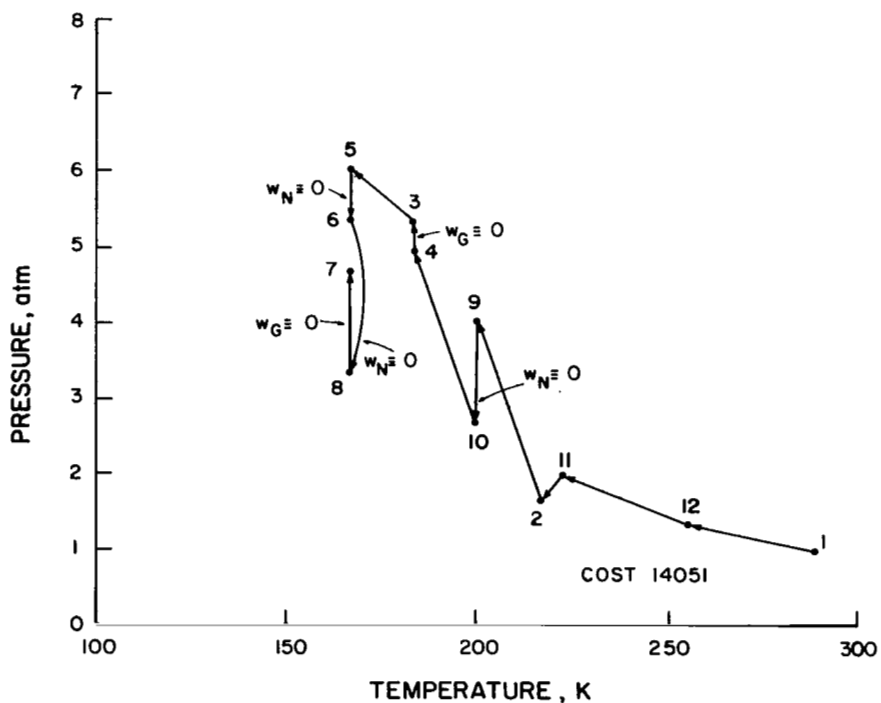fixed terminal set point at (167 K, 6.0 atm).

Figure 11.- Twelve-set-point optimum open tour with
fixed terminal set point at (167 K, 4.7 atm).

slightly reordered from the optimum closed tour. Figures 10 and 11 show open tours with fixed terminal set point for the same example. Since the tour of figure 10 terminates at (167 K, 6.0 atm) (the point of maximum pressure and minimum temperature), the algorithm is unable to take advantage of three transitions of decreasing pressure at constant minimum temperature, which results in a 20-percent increase in total cost over the optimum open tour with free terminal set point of figure 9. The open tour of figure 11 with fixed terminal set point at (167 K, 4.7 atm) is less expensive than that of figure 10 because of the two decreasing-pressure, constant-temperature transitions from (167 K, 6.0 atm) to (167 K, 5.3 atm) and then to (167 K, 3.3 atm) with $w_N \equiv 0$, even though the final transition is from (167 K, 3.3 atm) back up to (167 K, 4.7 atm). These runs demonstrate that open tours with fixed terminal set points should be selected carefully to avoid significantly higher operating costs.

CONCLUDING REMARKS

An algorithm for minimum-cost set-point ordering in a cryogenic wind tunnel has been developed. Efficient evaluation of state-transition costs is accomplished by means of a single-volume lumped model of wind-tunnel flow dynamics and the use of a high-performance numerical integration technique. Some idealized minimum-cost state-transition control strategies have been determined which provide the lowest attainable transition cost between set points. An operational set-point ordering procedure, which solves the "traveling salesman problem," is employed to determine the least costly ordering (tour) of a prespecified set of operating set points. These procedures have been organized into a preliminary software package for set-point ordering which is set up for National Transonic Facility wind-tunnel operating parameters. This software package has options for generation of optimum closed tours, open tours with free terminal set points, and open tours with fixed terminal set points. Numerical studies show that transitions which consume no liquid nitrogen coolant are highly favored because of their low cost. It is also shown that open tours with fixed terminal set points may be excessively costly and should be avoided.

APPENDIX

LOCAL OPTIMALITY OF ZERO-COOLANT TRANSITIONS

The state-transition cost J_L defined in equation (29) as a functional of the control law $L(w_N, w_G, P)$ is

$$J(w_N) = \int_{t_1}^{t_2} (P + rw_N)\, dt \tag{A1}$$

It is to be shown that if a transition along a fixed path between states (m_1, e_1) and (m_2, e_2) can be effected with $w_N \equiv 0$ then $J(w_N \equiv 0)$ is locally minimum along that path. Let δw_N denote a positive variation in w_N about $w_N \equiv 0$. It will be shown that the corresponding variation δJ is positive.

Let $g(m)$ be a differentiable function representing a transition path passing through points (m_1, e_1) and (m_2, e_2) for which $w_N \equiv 0$ in the (m, e) plane. Since m decreases monotonically with $w_N \equiv 0$ (inequality (49)) it follows that $g(m)$ must be a single-valued function. Along $g(m)$ equations (8) and (9) are

$$\dot{m} = w_N - w_G \tag{A2}$$

and

$$\dot{e} = g_m \dot{M} = h_N w_N - h_G w_G + P \tag{A3}$$

where

$$g_m = \frac{dg(m)}{dm} \tag{A4}$$

$$h_G = \frac{\gamma g(m)}{m + a_s} \tag{A5}$$

$$P = M^2 K_m \frac{\gamma - 1}{c_v V} m \left[\frac{g(m)}{m + a_s} \right]^{3/2} \tag{A6}$$

and M is a function of m and e. The transition cost is obtained from equations (29) and (A2) as

$$J(w_N) = \int_{m_1}^{m_2} \frac{P + rw_N}{w_N - w_G}\, dm \tag{A7}$$

Equations (A2) and (A3) are solved to obtain w_G in terms of w_N, h_G, and P, resulting in the following:

$$w_G = \frac{w_N (h_N - g_m) + P}{h_G - g_m} \qquad (A8)$$

Substituting equation (A8) into equation (A7) gives

$$J(w_N) = \int_{m_1}^{m_2} \frac{(P + rw_N)(h_G - g_m)}{w_N(h_G - h_N) - P}\, dm \qquad (A9)$$

Equation (A9) now provides the transition cost along transition path $e = g(m)$ as a functional of w_N independent of the transition time limits t_1 and t_2. The variation δJ of $J(w_N)$ about $w_N \equiv 0$, obtained by eliminating terms of order 2 and greater from the increment

$$\Delta J = J(w_N + \delta w_N) - J(w_N) \qquad (A10)$$

is found to be

$$\delta J \Big|_{w_N \equiv 0} = \int_{m_1}^{m_2} \delta w_N \frac{(r + h_G - h_N)(g_m - h_G)}{P}\, dm \qquad (A11)$$

Set $w_N \equiv 0$ in equations (8) and (9) and divide equation (9) by (8) to obtain the following:

$$g_m = \frac{de}{dm} = h_G - \frac{P}{w_G} < h_G \qquad (A12)$$

Since δw_N, r, h_G, and P are positive and h_N and Δm are negative, it follows from equation (A11) and inequality (A12) that δJ is positive.

REFERENCES

1. Balakrishna, S.: Minimum Energy Test Direction Design in the Control of Cryo-
   genic Wind Tunnels. NASA CR-163244, 1980.

2. Gumas, George: The Dynamic Modelling of a Slotted Test Section. NASA
   CR-159069, 1979.

3. Kirk, Donald E.: Optimal Control Theory - An Introduction. Prentice-Hall, Inc.,
   c.1970.

4. Bellmore, M.; and Nemhauser, G. L.: The Traveling Salesman Problem: A Survey.
   Oper. Res., vol. 16, no. 3, May-June 1968, pp. 538-558.

5. Little, John D. C.; Murty, Katta G.; Sweeney, Dura W.; and Karel, Caroline: An
   Algorithm for the Traveling Salesman Problem. Oper. Res., vol. 11, no. 6,
   Nov.-Dec. 1963, pp. 972-989.

6. Balas, Egon; and Christofides, Nicos: A Restricted Lagrangean Approach to the
   Traveling Salesman Problem. Management Sci. Res. Rep. No. 439 (Grant
   MCS76-12026 A02 and Contract N0014-75-C-0621 NR 047-048), Carnegie-Mellon
   Univ., July 1979. (Available from DTIC as AD A072 457.)

7. Whitehouse, Gary E.; and Wechsler, Ben L.: Applied Operations Research: A
   Survey. John Wiley & Sons, Inc., c.1976.

8. Henley, Ernest J.; and Williams, R. A.: Graph Theory in Modern Engineering.
   Academic Press, Inc., 1973.

9. Garfinkel, Robert S.; and Nemhauser, George L.: Integer Programming. John
   Wiley & Sons, Inc., c.1972.

10. Hindmarsh, A. C.: A Collection of Software for Ordinary Differential Equations.
    American Nuclear Society Proceedings of the Topical Meeting on Computational
    Methods in Nuclear Engineering - Vol. 3, Apr. 1979, pp. 8-1 - 8-15.

SYMBOLS

a	y-intercept of linear function, defined in equation (64)
a_s	$= (c_s/c_v) m_s$ (eq. (11))
C	transition-cost matrix
$\tilde{c}$	reference length, m
c_{ij}	transition cost from state s_i to state s_j
c_p	specific heat of gas at constant pressure, kJ/kg·K
c_s	specific heat of tunnel liner, kJ/kg·K)
c_v	specific heat of gas at constant volume, kJ/kg·K
e	total internal energy, kJ
G	$= \dfrac{RK_a}{Va}\left(\dfrac{V\lambda}{\gamma - 1} + a_s c_v\right)$ (eq. (71))
g(m)	single-valued function of m
g_m	first derivative of g(m), $\dfrac{dg(m)}{dm}$
h_G	enthalpy of vented gas, kJ/kg
h_N	enthalpy of LN$_2$, kJ/kg
I_s	index set
J	transition cost
J_L	transition cost of control L
J_Θ	total cost of tour Θ
K_a	constant, 9.87×10^{-3} atm/kPa
K_m	constant, 374.2 kW/atm·K$^{1/2}$
L	transition control
M	Mach number
m	total mass, kg
m_s	mass of tunnel liner, kg
N_{Re}	Reynolds number
P	fan power, kW

p	static pressure, atm (1 atm = 101.3 kPa)
q	dynamic pressure, kPa
R	gas constant, kJ/kg·K
r	ratio of LN_2 cost to fan-energy cost, 7.886×10^6 kJ/kg
S	set of set points
s	set point
T	static temperature, K
t	time, sec
V	volume of tunnel, m^3
w_G	gas-vent flow rate, kg/sec
w_N	LN_2 injection flow rate, kg/sec
γ	ratio of specific heats
Δ	increment
δ	variation
Θ	closed tour
Θ_o	open tour
λ	slope of linear function, defined in equation (61)
μ	viscosity, $N \cdot sec/m^2$
ρ	density, kg/m^3
Ω	transition set

Subscripts:

max	maximum
min	minimum
t	total value
1	initial state
2	final state

A dot over a symbol indicates differentiation with respect to time. A prime denotes a particular value of a variable. An asterisk denotes an optimum function or value.

1. Report No.	2. Government Accession No.	3. Recipient's Catalog No.
NASA TP-1923		

4. Title and Subtitle	5. Report Date
AN ALGORITHM FOR MINIMUM-COST SET-POINT ORDERING IN A CRYOGENIC WIND TUNNEL	November 1981
	6. Performing Organization Code
	505-31-63-03

7. Author(s)	8. Performing Organization Report No.
John S. Tripp	L-14695
	10. Work Unit No.

9. Performing Organization Name and Address	
NASA Langley Research Center Hampton, VA 23665	11. Contract or Grant No.
	13. Type of Report and Period Covered

12. Sponsoring Agency Name and Address	Technical Paper
National Aeronautics and Space Administration Washington, DC 20546	14. Sponsoring Agency Code

15. Supplementary Notes

16. Abstract

An algorithm for minimum-cost ordering of set points in a cryogenic wind tunnel is developed. The procedure generates a matrix of dynamic state-transition costs, which is evaluated by means of a single-volume lumped model of the cryogenic wind tunnel and the use of some idealized minimum-cost state-transition control strategies. A branch and bound algorithm is employed to determine the least costly sequence of state transitions from the transition-cost matrix. Some numerical results based on data for the National Transonic Facility are presented which show a strong preference for state transitions that consume no coolant. Results also show that the choice of the terminal set point in an open ordering can produce a wide variation in total cost.

17. Key Words (Suggested by Author(s))	18. Distribution Statement
Set-point ordering Wind tunnel Simulation Cost minimization	Unclassified - Unlimited
	Subject Category 09

19. Security Classif. (of this report)	20. Security Classif. (of this page)	21. No. of Pages	22. Price
Unclassified	Unclassified	30	A03

National Aeronautics and
Space Administration

Washington, D.C.
20546

THIRD-CLASS BULK RATE

U.S.MAIL

NASA

POSTMASTER: If Undeliverable (Section 158
Postal Manual) Do Not Return